Nuclear Materials and Energy 12 (2017) 786–790

Contents lists available at ScienceDirect

Nuclear Materials and Energy

journal homepage: www.elsevier.com/locate/nme

EDGE2D-EIRENE simulations of the impact of poloidal flux expansion on the radiative divertor performance in JET

B. Viola[a,*], G. Calabró[a], A.E. Jaervinen[b], I. Lupelli[c], F. Maviglia[d], S. Wiesen[e], M. Wischmeier[f], JET Contributors[g,1]

[a] ENEA, C.R. Frascati, Via E. Fermi 45, Frascati (Rome) 00044, Italy
[b] Lawrence Livermore National Laboratory, Livermore, CA 94550, USA
[c] Culham Centre of Fusion Energy, Abingdon OX14 3DB, UK
[d] Consorzio CREATE, Univ. Napoli Federico II - DIETI, Napoli 80125, Italy
[e] Forschungszentrum Jülich GmbH, Institut für Klima-und Energieforschung - Plasmaphysik, 52425 Jülich, Germany
[f] Max-Planck-Institut fuer Plasmaphysik, Boltzmannstr. 2, Garching D-85748, Germany
[g] EUROfusion Consortium, JET, Culham Centre of Fusion Energy, Abingdon OX14 3DB, UK

ARTICLE INFO

Article history:
Received 18 January 2017
Revised 12 June 2017
Accepted 9 July 2017
Available online 17 July 2017

Keywords:
Power exhaust
Radiation
EDGE2D
EIRENE
JET
Nitrogen
Impurity seeding

ABSTRACT

In the past at JET, with the MkI divertor, a systematic study of the influence of X-point height and poloidal flux expansion has been conducted [1,2] showing minor differences in the radiation distribution, whereas in [3] experiment and simulations have shown enhancement of detachment as the flux expansion was increased. More recently at JET, equipped with the ITER-like wall (ILW), radiative seeded scenarios have been studied and a maximum radiation fraction 75% has been achieved. EDGE2D-EIRENE [4–6] simulations [7,8] have already shown that the divertor heat fluxes can be reduced with N2 injection, qualitatively consistent with experimental observations [9], by adjusting the impurity injection rate to reproduce the measured divertor radiation. In this paper we will present edge predictive simulations on the assessment of effects of poloidal flux expansion and recycling on radiation distribution and X-point peaking on JET-ILW nitrogen seeded plasmas.

1. High flux expansion plasmas

For a burning plasma device like ITER, radiative power removal by seeded impurities will be inevitable to avoid divertor damage. Increasing divertor radiation by injecting low-Z impurities such as nitrogen, to reduce scrape-off layer heat flux and to cool the divertor plasma to detachment, is put forward as the primary method to achieve this goal. Here, the possibility of increasing the radiative fraction is assessed by using poloidal magnetic flux expansion.

Semi-horizontal configurations, as discussed in [10], have been modified below the X-point position by keeping the plasma boundary unchanged [11]. A reference equilibria has been designed from *JPN* 81472 @ $t = 9$ s lowering the inner strike point and moving outwards the outer strike point (on stack D), Fig. 1. The modified magnetic configurations, with inner strike point located on inner vertical target and outer one on full tungsten horizontal target, have been designed to increase similarly flux expansion on both inner and outer target. Fig. 1 shows the high flux expansion (HFE) equilibria. Table 1 gives a summary of the flux expansion, for the analysed cases.

Fig. 1(a) shows the three equilibria used on EDGE2D–simulations: the reference (REF) equilibrium and two high flux expansion (HFE) equilibria. Recently [11], HFE experimental ohmic discharges have been obtained at JET and reported on Fig. 1(b) confirming the predictions on the increase of flux expansion (both on X-point and targets) discussed in Table 1. Two different flux expansion are calculated in the following way: the flux expansion on the inner/outer target is the distance between the strike points of the Scrape Off-Layer (SOL) boundary and of the separatrix along the target tile on the poloidal plane.

It should be noted that the due to the limitations on position and polarities of the divertor coils, as discussed in [11], only a maximum increase ~20% on X-point outwards and ~50% on outer target can be obtained. In order to distinguish the effects on the divertor radiation due to a possible higher recycling contribution

* Corresponding author.
E-mail address: bruno.viola@enea.it (B. Viola).
[1] See the author list of "X. Litaudon et al. 2017 Nucl. Fusion 57 102001".

http://dx.doi.org/10.1016/j.nme.2017.07.004

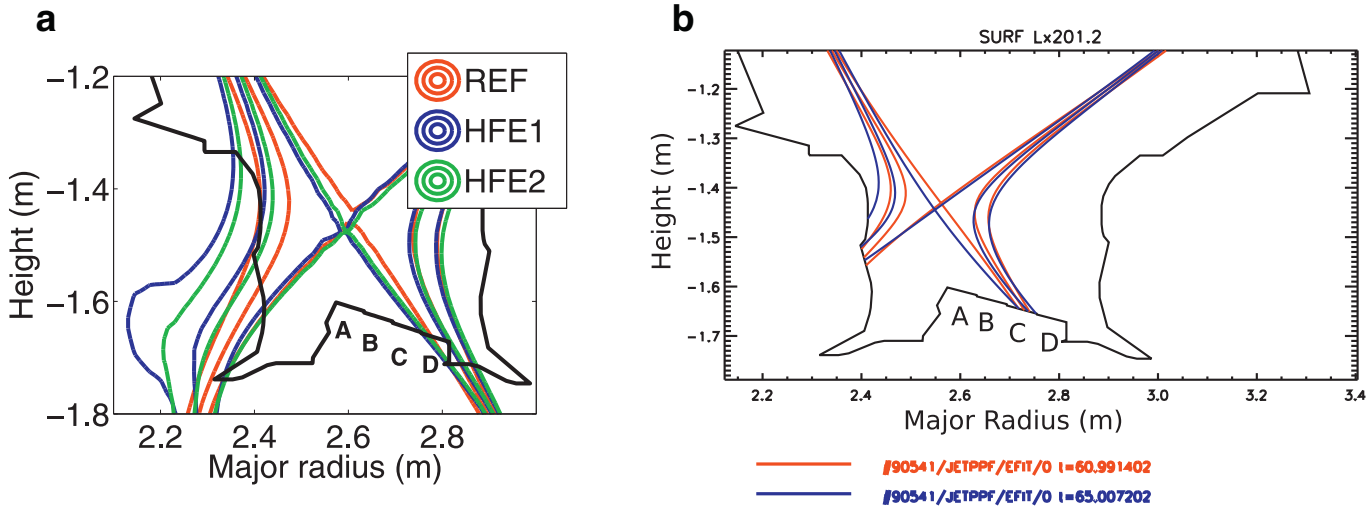

Fig. 1. Figure a shows the three equilibria used for the analysis: we will refer to the red solid line as reference (REF), the blue dotted one as HFE1, the green dash-dotted one as HFE2, which differentiates from the former HFE1 as it should minimize recycling contribution to radiation from the interaction with the inner wall. In figure b in red and in blue experimental REF (*JPN* 90541 @ $t = 21$ s) and HFE (*JPN* 90541 @ $t = 25$ s) equilibria are depicted respectively. Letters define the four stacks of the horizontal tile. (For interpretation of the references to colour in this figure legend, the reader is referred to the web version of this article.)

Table 1
Flux Expansion on the X-point plane and on the inner and outer targets: the subscript *exp* refers to data collected from JPN 90541.

	$X_p\|_{IN}$	$X_p\|_{OUT}$	$Target\|_{IN}$	$Target\|_{OUT}$
REF_{exp}	35.46	36.46	6.21	4.09
HFE_{exp}	42.03	44.11	12.73	5.93
REF	32.44	34.61	4.62	3.61
HFE1	37.51	41.68	9.86	4.49
HFE2	36.44	40.76	8.36	4.41

from the interaction with the inner wall, the inner target to X-point distance are different in the two modified equilibria (HFE1 and HFE2 in Fig. 1a): HFE2 equilibrium is ~2 cm away from the inner target tile.

2. EDGE2D-EIRENE setup

EDGE2D-EIRENE was executed for steady-state nitrogen seeded simulations for these equilibria to predict radiation distributions and divertor conditions. Simulations were performed to assess the hierarchy of the physics processes and the impact of the divertor geometry on the radiative divertor performance. The main boundary conditions presented here are those used in [7] where the radiation properties of H-mode nitrogen seeded plasmas are studied. The input power was set to 8 MW corresponding to the experimentally estimated power crossing the separatrix between Edge Localized Modes (ELMs): 7 ~ 9 MW. In the divertor plasma below the X-point radially constant heat conductivities ($1\,m^2/s$) and particle diffusivities ($0.64\,m^2/s$) were imposed. The deuterium fuelling levels are adjusted individually for the three configurations to provide the same outer mid-plane separatrix electron density $n_{e,sep,LFS-MP}$. After this step, the deuterium fuelling, puffed from the divertor common SOL, is kept fixed throughout the nitrogen seeding scans and, as a result, the $n_{e,sep,LFS-MP}$ is floating in the simulations. Beryllium is considered not recycling whereas nitrogen is assumed to be fully recycling. This assumption for nitrogen is one of the two options available in the code and may lead to overestimate radiative values, as found in [7]. Tungsten is not included. The nitrogen content in the computational domain is feedback controlled to provide requested levels of nitrogen radiated power in the simulations: 0, 3, 5, and 6 MW. The feedback puff is located in the low field side (LFS) above the divertor to minimize the impact of the feedback on the LFS divertor characteristics analyzed in this study. With the full recycling assumption, the nitrogen source distribution is primarily regulated through the recycling source and the details of the gas puff are of minor importance. For neutral atoms and molecules, and impurity atoms, the Kotov-2008 neutral physics setup [12] was used which includes a more extensive set of elastic and inelastic collisions between deuterium ions and molecules, and molecular dissociation of D_2, and thus represents a better description of divertor conditions near detachment. Cross-field drifts ($E \times B$ and $B \times \nabla B$) are not included in these simulations, due to numerical stability, their use is postponed to a future work. Even though experimental studies [13] suggest that divertor asymmetries are sensitive to cross-field drifts, drifts are more efficient in varying density and temperature at the inner target [14]: for these reasons the analysis focuses on the LFS divertor only, less prone to such effects.

3. Unseeded plasmas

In the unseeded plasmas, the code predicts for the three divertor configurations similar main SOL and pedestal electron density and temperature profiles at the outer mid-plane. Outer target temperature and peak saturation currents is the same within about 5% in all the configurations throughout the density scan performed from $n_{e,sep,LFS-MP}$ equal 3×10^{19} to $7 \times 10^{19}\,m^{-3}$ feedback controlling the density. In the plasmas without extrinsic impurity seeding the ionization distribution for the HFE1 and HFE2 cases are radially broader than the reference case which has a distribution localized in front of the strike point: the neutral distribution recycle towards the far SOL producing broader ionization distribution. On the other hand, neutrals are predicted to be better confined in HFE2, leading to lower neutral currents crossing the separatrix (Fig. 2c) and, subsequently, to ~10% lower CX losses in the core Fig. 2b, peak T_e is the same within about 5% in all the configurations, Fig. 2d. Simulations also predict a slightly higher pumping rate Fig. 2a, which in turn, leads to an increased ϕ_{puff} required to reach the requested $n_{e,\,sep,\,LFS-MP}$. The increased neutral penetration in HFE1 respect to HFE2 is caused by a reduced X-point to target distance, [15]. The total power flowing in the outer divertor is similar for the three configurations, although the $Q_{\|,\,LFS}$ is greater

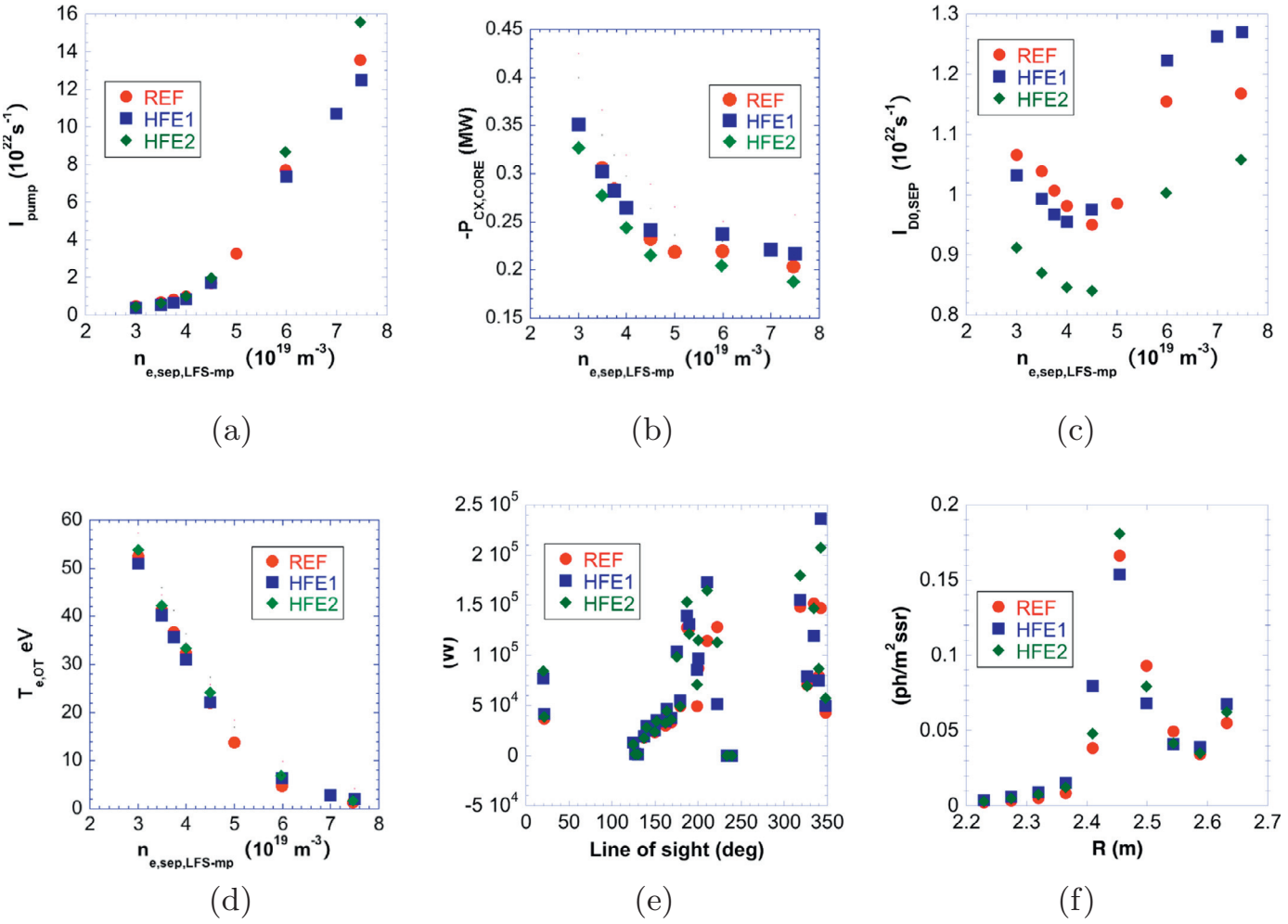

Fig. 2. (a) $I_{Div,\ LFS}$, (b) charge exchange loss power in the core, (c) total atomic deuterium current across separatrix, (d) $T_{e,peak,LFS\text{-}plate}$, (e) EDGE2D-EIRENE predictions of the KB5 bolometer line integrated radiated power for $n_{e,sep,LFS\text{-}MP} = 4.5 \times 10^{19}$ m^{-3}, and (f) predicted divertor D_α-emission at the same density.

for the HFE1 equilibrium ($\sim 7 \times 10^7$ W, $\sim 6.5 \times 10^7$ W, $\sim 6 \times 10^7$ W for HFE1, HFE2 and REF, respectively). This is caused by a more favourable inclination angle of the field line to the plate in this configuration than the reference. In these plasmas the divertor radiation predicted levels favour the configurations with high flux expansion: the slight increase is due to atomic and molecular processes and charge exchange, enhanced for these equilibria, which in turn can be attributed to an increased connection length. The increase in radiated power with respect to the reference case is $\sim$15%, when considering the entire divertor radiation: as the synthetic bolometer predictions are concerned the increase of radiation around the X-point is $\sim$50% (Fig. 2e). Similar to the radiated power, the overall LFS divertor D_α emission (Fig. 2e) is increased in the modified shapes by $\sim$20%. The peak LFS divertor D_α emission is reached at the LFS strike point in the HFE configurations. HFE1 and HFE2 configurations show more D_α emission in the LFS divertor leg, whereas at the high field side (HFS) the HFE2 equilibria is predicted to emit less than HFE at the inner target baffle: the recycling for this configuration looks lower than HFE1 for the same upstream plasma conditions. This is also confirmed by the particle flux to the target profiles.

4. Nitrogen seeded simulations

In the nitrogen radiation controlled simulations, the total power flowing in the outer divertor is unchanged for the three configurations. When N is puffed in the simulation domain, a $\sim$ 10% lower power density is predicted for HFE equilibrium. In the simulations with floating $n_{e,sep,LFS\text{-}MP}$, for all the magnetic configurations considered in this report, $n_{e,sep,LFS\text{-}MP}$ is reduced nonlinearly from 4.5×10^{19} m^{-3} to 3.8×10^{19} m^{-3} within the seeding scan. To address the uncertainties in $n_{e,sep,LFS\text{-}MP}$, simulations with $n_{e,sep,LFS\text{-}MP}$ fixed to 4.5×10^{19} m^{-3} with deuterium feedback control were conducted showing no substantial differences on divertor conditions, same conclusions were drawn in [8] for the horizontal LFS divertor configuration. EDGE2D-EIRENE predicts that fairly similar SOL radiation fractions of 50–60% are needed in both configurations with high flux expansion to reach LFS divertor peak heat fluxes less than 2 MW/m^2. Furthermore, a factor 10 reduction in the LFS target power deposition with increasing divertor radiation is predicted by the code in the high-seeded case respect to the unseeded case. This corresponds to an increase of the normalized divertor radiation, $P_{rad,\ divertor}/P_{SOL}$ from the unseeded levels of 10% up to the 50%, as also observed in [8].

When comparing the radiative characteristic of the three configurations, EDGE2D-EIRENE predicts, for similar divertor radiation fraction, a reduction of the nitrogen concentration needed to obtain a given radiation level is predicted by the code, Fig. 3a. The simulated nitrogen concentration into the computational domain is $\sim$20% lower in the high flux expansion equilibria HFE1 than the reference case; for the same level of N radiation, $Z_{eff,\ ped}$ is the same within about 5% in all the configurations. As the nitro-

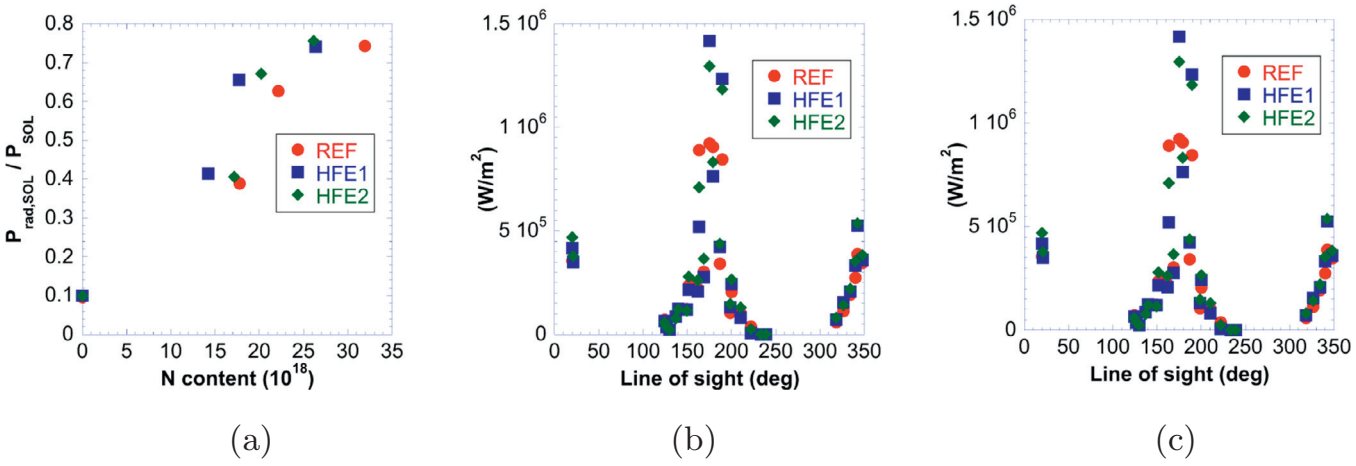

Fig. 3. (a) SOL radiation fraction $P_{rad,\,SOL}/P_{SOL}$, (b) predicted radiation from the divertor bolometer, (c) predictions of the KB5 vertical bolometer line integrated radiated power in the feedforward fuelled simulations. X-point is located at $R = 2.55$ cm.

gen is puffed in the domain, qualitatively all configurations show the same behaviour: a factor of 2 increase is predicted in the LFS divertor radiated power, with the peak of the radiation distribution located in front of the target plate. Simultaneously, transition to high recycling conditions is observed at the LFS divertor as the peak electron temperature drops from 20 eV to 10 eV. With medium N2 injection, a further ~50% of radiated power increase is observed in the LFS divertor leg with a simultaneous shift of the peak emission zone from the LFS strike point to the LFS X-point, while the plasma conditions in the LFS divertor remained in high recycling regime. The broad ionization distribution in front of the outer strike point moves from the SOL towards the X-point. Simultaneously, the peak LFS target saturation current is reduced to $1.87 \times 10^{24}\,s^{-1}m^{-2}$ transition to semi-detached divertor conditions. At high N2 injection the temperature profiles are flat, ~ 1 eV and the ionization front detaches from the strike point, the saturation current profile is reduced uniformly across the profile, leading to a gradual divertor profile detachment as described in [8,16]. The total power deposition at the LFS divertor is reduced by a factor 3–5 in high recycling conditions compared to the unseeded simulations. Fig. 3b shows that the modified equilibria radiate more near the X-point than the reference, a factor ~2 when 5 MW nitrogen radiation is considered. As for the D_α emission as the nitrogen content increases a shift of the deuterium ionization front towards the X-point, a decrease of the emission for all equilibria is predicted to occur at the LFS. The finding in these studies appears to be inconsistent with the increase in D_α emission with degree of detachment in unseeded L-mode ([17], Fig. 11l) and H-mode ([8], Fig. 14a) plasmas, further analysis is ongoing.

Using this setup, the impact of divertor geometry on the radiative characteristics in these plasmas confirm findings of [10]. For this reason the equilibria have been compared applying also a feedforward nitrogen seeding scheme. Applying a seeding rate of 2.65×10^{20} part/s, the nitrogen radiated power in the reference equilibrium is 4 MW, which yields a divertor radiation of ~ 2.8 MW. The total radiation for all HFE cases is ~40% and ~30% higher for HFE1 and HFE2, respectively. In the modified equilibria there is a broadening of the ionization front into the SOL, which follows the temperature contour. In particular EDGE2D-EIRENE predicts the divertor radiation to be dominated by the HFS component in the HFE equilibria. Both divertor and vertical predicted bolometer radiated powers favour the HFE1 configuration, Fig. 3, the radiation increase is more pronounced in the vicinity of the X-point by approximately ~50%. The effect of a lower recycling in HFE2 can be seen from the vertical bolometer data: since the nitrogen source distribution is dominated by the recycling source, which is a function of nitrogen content in the plasmas, we see a lower nitrogen radiation for the HFE2 case: it is still not clear if it is due to the lower nitrogen content or if there is a recycling effect on radiation. Generally HFS conditions are difficult to investigate especially when drifts are omitted [10]; our current understanding is that we improvements in the code to recover LFS/HFS asymmetries, i.e. need for cross-field drifts, a neutral model that includes also the transport through gaps and leaks and a non diffusive model for the edge plasma [18].

5. Conclusions

Radiative divertor operation in nitrogen seeded, high-triangularity JET H-mode plasmas with various levels of poloidal flux expansion in semi-horizontal configuration have been simulated with the multi-fluid code EDGE2D-EIRENE. Flux expansion modified equilibria are predicted to radiate ~ 15% more in the vicinity of the X-point and have a ionization front extending further in the SOL than the reference equilibrium. Moreover, HFE cases offer a benefit in reducing by 20% the nitrogen concentration needed to obtain a given radiated power level. Simulations have also shown that equilibria with lower recycling yield a lower radiation but at the moment, there are no indications on how to disentangle the effect of inner target recycling on the divertor radiation.

Acknowledgements

This work has been carried out within the framework of the EUROfusion Consortium and has received funding from the Euratom research and training programme 2014–2018 under grant agreement no. 633053. The views and opinions expressed herein do not necessarily reflect those of the European Commission.

References

[1] C. Lowry, et al., Divertor configuration studies on jet, J. Nucl. Mater. 241–243 (1997) 438–443.
[2] A. Loarte, et al., Plasma detachment in JET mark i divertor experiments, Nucl. Fusion 38 (3) (1998) 331–371, doi:10.1088/0029-5515/38/3/303.
[3] R. Pitts, et al., Divertor geometry effects on detachment in TCV, J. Nucl. Mater. 290–293 (2001) 940–946, doi:10.1016/S0022-3115(00)00461-X.
[4] R. Simonini, et al., Models and Numerics in the Multi-Fluid 2-D Edge Plasma Code EDGE2D/U, Contrib. Plasma Phys. 34 (1994) 368–373.
[5] D. Reiter, Progress in two-dimensional plasma edge modelling, J. Nucl. Mater. 196–198 (C) (1992) 80–89, doi:10.1016/S0022-3115(06)80014-0.

[6] S. Wiesen, et al., Technical report, 2006. http://www.eirene.de/e2deir_report_30jun06.pdf.
[7] A. Jaervinen, et al., Interpretation of radiative divertor studies with impurity seeding in type-i ELMy H-mode plasmas in JET-ILW using EDGE2D-EIRENE, J. Nucl. Mater. 463 (2015) 135–142, doi:10.1016/j.jnucmat.2014.10.047.
[8] A. Jaervinen, et al., Impact of divertor geometry on radiative divertor performance in JET H-mode plasmas, Plasma Phys. Controlled Fusion 58 (4) (2016), doi:10.1088/0741-3335/58/4/045011.
[9] C. Giroud, et al., Progress at JET in integrating ITER-relevant core and edge plasmas within the constraints of an ITER-like wall, Plasma Phys. Control. Fusion 57 (035004) (2015).
[10] M. Groth, et al., Divertor plasma conditions and neutral dynamics in horizontal and vertical divertor configurations in JET-ILW low confinement modeplasmas, J. Nucl. Mater. 463 (2015) 471–476.
[11] G. Calabrò, et al., Divertor configuration with two nearby poloidal field nulls: modelling and experiments for EAST and JET tokamaks, in: Proc. of the 22nd PSI Conference on Plasma Surface Interaction, Rome, Italy, May 30th–June 3rd, 2016.
[12] V. Kotov, et al., Numerical modelling of high density jet divertor plasma with the SOLPS4.2 (B2-EIRENE) code, Plasma Phys. Controlled Fusion 50 (10) (2008), doi:10.1088/0741-3335/50/10/105012.
[13] R. Pitts, et al., Edge and divertor physics with reversed toroidal field in JET, J. Nucl. Mater. 337–339 (1–3 SPEC. ISS.) (2005) 146–153, doi:10.1016/j.jnucmat.2004.10.111.
[14] A. Chankin, et al., Interpretation of SOL flows and target asymmetries in JET using EDGE2D code calculations, J. Nucl. Mater. 290–293 (2001) 518–524, doi:10.1016/S0022-3115(00)00516-X.
[15] D. Moulton, et al., Pumping in vertical and horizontal target configurations on JET in L-mode; pumping in vertical and horizontal target configurations on JET in L-mode; an interpretive study using EDGE2D-EIRENE, in: Proc. of the 42nd EPS Conference on Plasma Physics, Lisbon, Portugal, 22nd–26th of June, 2015.
[16] A. Kallenbach, et al., Partial detachment of high power discharges in ASDEX upgrade, Nucl. Fusion 55 (5) (2015), doi:10.1088/0029-5515/55/5/053026.
[17] M. Groth, et al., Impact of carbon and tungsten as divertor materials on the scrape-off layer conditions in JET, Nucl. Fusion 53 (2013) 093016.
[18] S. Wiesen, et al., Plasma-edge and plasma-wall interaction modelling: lessons learned from metallic devices, in: Proc. of the 22nd PSI Conference on Plasma Surface Interaction, Rome, Italy, May 30th–June 3rd, 2016.